Growth and photoluminescence of vertically aligned ZnO nanowires/nanowalls

Growth and photoluminescence of vertically aligned ZnO nanowires/nanowalls

Fang Fang[1,2]**, Dongxu Zhao**[1,3]**, Binghui Li**[1]**, Zhenzhong Zhang**[1]**, Jiying Zhang**[1] **and Dezhen Shen**[1]

[1] Key Laboratory of Excited State Processes, Changchun Institute of Optics, Fine Mechanics and Physics, Chinese Academy of Sciences, 16 East Nan-Hu Road, Open Economic Zone Changchun 130033, People's Republic of China
[2] Graduate School of the Chinese Academy of Sciences, People's Republic of China

E-mail: dxzhao2000@yahoo.com.cn

Abstract
By controlling the incoming gas flow, vertically aligned ZnO nanowires and nanowalls have been successfully synthesized on a Si (1 0 0) substrate by the simple physical vapour deposition method. The growth process of the ZnO nanowalls was observed by adjusting the growth time. The probable growth mechanisms of the ZnO nanowires and nanowalls were discussed in detail. In contrast to the photoluminescence results of nanowires, an enhancement of the LO phonon signal was observed in ZnO nanowalls, which was attributed to an additional channel of electron–phonon coupling induced by the residual strains in the ZnO nanowalls during the coalescence growth process.

(Some figures in this article are in colour only in the electronic version)

The applications of nanostructured materials in microelectronic and optoelectronic devices are one of the major focuses in recent nanoscience research [1–3]. Among these, ZnO nanostructures have attracted particular attention because of their unique properties (a direct band gap of 3.37 eV and a large exciton binding energy of 60 meV at room temperature) and diverse nanostructures. There has already been much progress in the synthesis of low-dimensional ZnO nanostructures, such as nanowires [4], nanobelts [5], nanorods [6] and nanotubes [7]. The successful synthesis of these diverse nanostructures opens numerous fields of application. For example, field-effect transistors, solar cells and light-emitting diodes have been realized based on ZnO nanostructures. As a different form of the above ZnO nanostructures, in particular, its two-dimensional structure, the nanowall may provide an excellent opportunity for physicists to explore new physics of ZnO nanostructures with open boundaries [8–10].

In this work, we report vertically aligned ZnO nanostructures (nanowires and nanowalls) grown on the Si (1 0 0) substrate by using a simple physical vapour deposition method. Unlike the previous fabrication methods using Au as a catalyst [11, 12], we deposited a thin ZnO film on the Si substrate as the nucleation site, which not only avoids contamination from the metal catalysts but also controls the growth direction of ZnO nanostructures. Fang's group has used this method to synthesize vertically aligned ZnO nanorod–nanowall junction arrays on a ZnO-coated silicon substrate [13] and has shown good results. By controlling the incoming gas flow, we could realize the conversion from 1D nanowires to 2D nanowalls. Except for the difference in morphology, photoluminescence (PL) of both nanostructures also shows a significant distinction. In addition, a detailed understanding of the probable growth mechanisms of the ZnO nanowires and nanowalls is presented.

The ZnO nanostructures were fabricated via a simple vapour-phase transport process. The highly c-axis-oriented ZnO template layer (100 nm thick) was deposited on the Si substrate surface by electron beam evaporation at 400 °C. Neither catalysts nor additives were used in this experiment. A mixture of commercial ZnO and graphite powders at a certain weight ratio of 1 : 1 served as a source material. A quartz

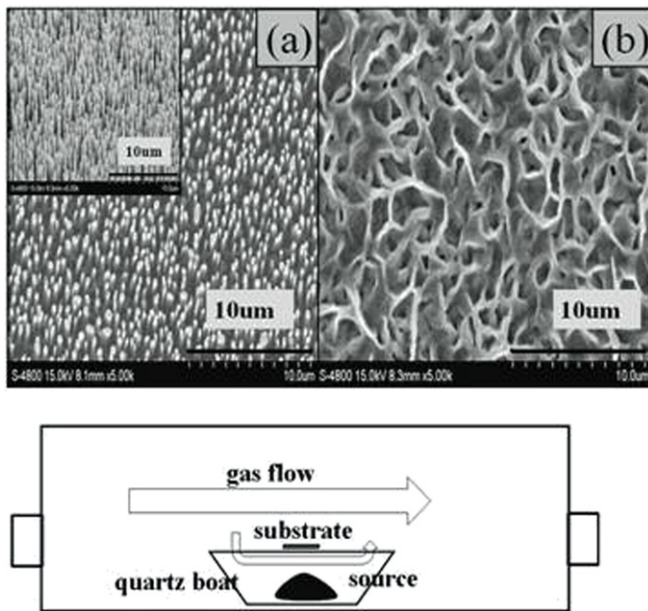[3] Author to whom any correspondence should be addressed.

Figure 1. The top view FESEM images of (*a*) sample A—ZnO nanowires and (*b*) sample B—ZnO nanowalls, the inset image shows the tilted (45°) view of sample A; the inset shows the schematic diagram of the setup.

boat containing both the powder mixture and the (ZnO/Si) substrates (laid ZnO side face-down above the source material with a vertical distance of 4 mm) was first placed in the central hot zone inside a horizontal quartz tube furnace (the inset of figure 1 shows the schematic diagram of the setup). After the Ar gas was introduced into the quartz tube and kept for 1 h to drive the residual air away, the furnace was heated up to the desired temperature. The whole experiment was under the protection of a constant flow of Ar (99.99%) with a flow rate of 100 sccm. By changing the incoming oxygen flow, two types of nanostructures with different morphologies were obtained labelled A and B, respectively. For sample A, the furnace was heated up to the desired temperature at 990 °C under a constant flow of Ar of 100 sccm at a rate of 30 °C min^{-1} and kept at 990 °C for 30 min. To grow sample B, oxygen was introduced into the furnace with a flow rate of 10 sccm once the temperature was raised to 990 °C. After growth, both substrates were cooled down to room temperature naturally under the forming gas. A white grey layer was found on the surface of the substrate. And then the samples were investigated by field-emission scanning electron microscopy (FESEM) and x-ray diffraction (XRD). Photoluminescence (PL) measurement was performed using a He–Cd laser line of 325 nm as excitation source. The morphologies of the two samples on the ZnO/Si substrate are shown in figure 1. Aligned ZnO nanowires are found for sample A (as shown in figure 1(*a*)). The ZnO nanowires have diameters ranging from 50 to 120 nm and lengths around 5 μm. Figure 1(*b*) shows a typical SEM micrograph of sample B. Two-dimensional ZnO nanowalls interconnect each other and form a random honeycomb-like template, which are serpentine with random curvature on the substrate. The nanowalls are about 200–300 nm thick and 1 μm high, whereon some stripes stand upright.
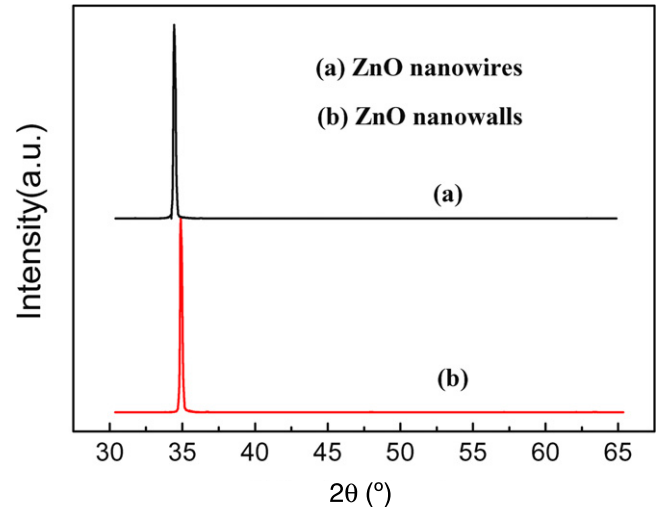

Figure 2. XRD results of (a) sample A—ZnO nanowires and (b) sample B—ZnO nanowalls.

Figure 2 shows the x-ray diffraction (XRD) spectra of the as-grown samples. As can be seen in the spectra, only the hexagonal ZnO (0 0 2) diffractive peak appears, suggesting the fully *c*-axis preferred orientation for both the samples (the *c*-plane parallel to the substrate). This result is in agreement with the SEM image. Compared with ZnO bulk materials ($2\theta = 34.42°$), the (0 0 2) diffractive peaks of ZnO nanowires and nanowalls are located at 34.45° and 34.63°, respectively. Obviously, the (0 0 2) position of the ZnO nanowalls has a larger deviation from the bulk. It is suggested that the *c*-axis orientation is compressed and the *a*-axis orientation stretched during the growth process of the nanowalls. A detailed explanation is provided below.

Based on our previous report [14], the growth of nanowires followed a vapour transport solid condensation mechanism with the ZnO film acting as a seed layer for nucleation. The ZnO nuclei were formed from the oxidation of zinc vapour, which was produced by the carbonthermal reduction of ZnO powder. This mechanism could also be applied to the growth of ZnO nanowalls. To analyse the growth mechanism of ZnO nanowalls, we have grown another three samples using the same growth condition as sample B except for different growth times: 5 min, 10 min, 20 min and 30 min (sample B) corresponding to figures 3(*a*)–(*d*), to directly observe the growth process. Based on the morphology changing process, we can describe the growth of the nanowalls in three parts: nucleation, grow up and combination. In the initial period, ZnO nanowalls nucleate and incubate a bigger rod-like ZnO seeding layer with the *c*-axis preferred orientation on the surface of ZnO thin film (figure 3(*a*)). With increasing growth time, these nanorods combine together to complete the in-plane grain growth (figure 3(*b*)). Further, two-dimensional ZnO nanowalls interconnect each other and form a random honeycomb-like template (figures 3(*c*) and (*d*)). In contrast to the experimental conditions of 1D nanowires, we just change one parameter (the incoming gas flow) to obtain completely 2D nanowalls. The influence of changing the incoming gas flow is important because it can change the relative gas concentration inside the tube, especially when the amount of oxygen in the
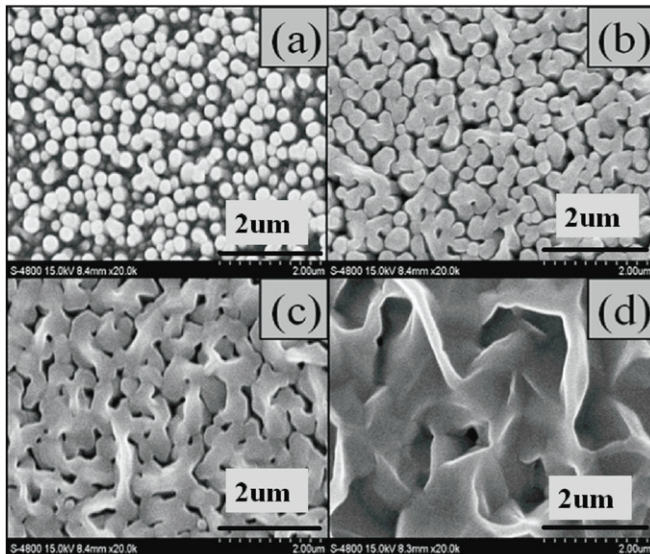
Figure 3. FESEM images of the sample B-ZnO nanowalls (*a*) for 5 min, (*b*) for 10 min, (*c*) for 20 min and (*d*) for 30 min growth.
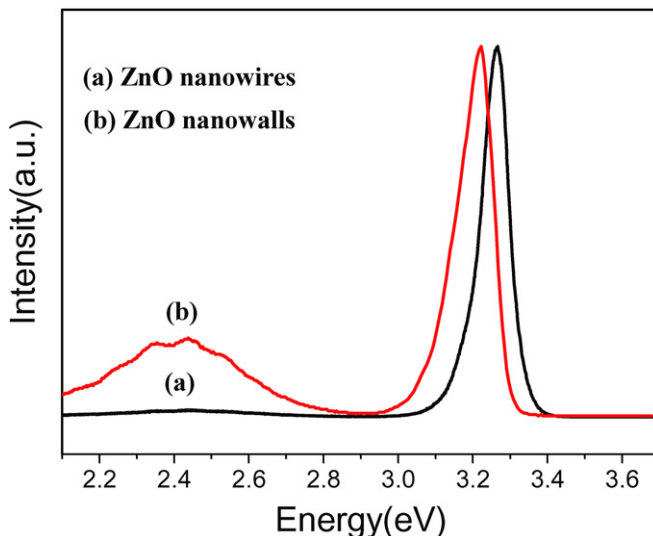

Figure 4. Room temperature PL spectrum of (a) sample A—ZnO nanowires and (b) sample B—ZnO nanowalls.

Figure 5. PL spectra of the ZnO nanowires measured at different temperatures (from 83 to 275 K): (*a*) sample A—ZnO nanowires and (*b*) sample B—ZnO nanowalls.

incoming gas is changed [15]. The variation in the oxygen partial pressure directly affects the process of reoxidation of the Zn vapour and the growth characteristics. The extra induced oxygen may create a greater concentration of growth species by oxidizing the Zn vapour more quickly [16]. This would lead to a higher supersaturation, which promotes two-dimensional growth mode.

Figure 4 shows the room temperature PL spectra of sample A and sample B. The PL spectra of both samples are composed of two main parts: one is an excitonic emission with energy around the band gap of ZnO in the ultra-violet (UV). The peaks of the nanowires and the nanowalls are located at 3.26 eV (380 nm) and 3.23 eV (384 nm), respectively. The other is the defect-related deep-level emission in the visible range. The deep-level emission at around 2.43 eV (510 nm) is commonly believed to come from the singly ionized oxygen vacancy or surface states [17, 18].
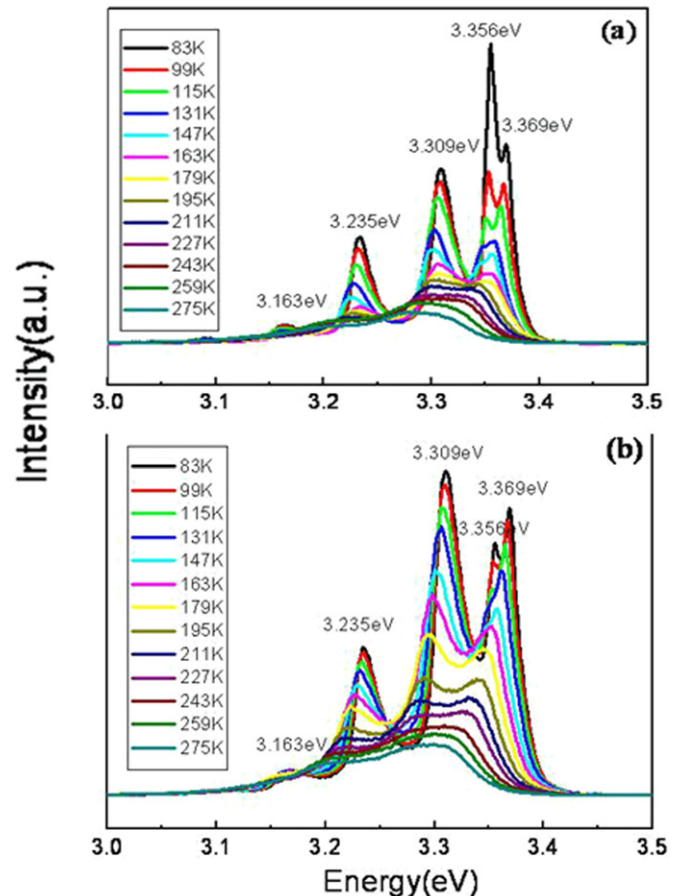
To analyse the origin of the UV emission peaks, the PL measurements of the two samples were performed in temperatures ranging between 83 and 275 K. At 83 K, the PL spectrum of the ZnO nanowires shows various peaks located at 3.369 eV, 3.356 eV, 3.309 eV, 3.235 eV and 3.163 eV, respectively, as shown in figure 4(a). The dominant peak at 3.356 eV and its shoulder (at the higher energy) at 3.369 eV can be assigned to a neutral donor bound exciton (D_0X) and a free-exciton (FX) emission. At the lower-energy position of D_0X, two emission peaks emerge, which are considered to be the phonon replicas of FX. Here, the energy separation of FX-1LO is smaller than the LO phonon energy (72 meV) due to the energy softening of FX-1LO [19]. Compared with nanowires, the peak position of the nanowalls remained nearly unchanged. However, for the luminous intensity, the FX recombination of nanowires is stronger than its phonon replica at 83 K. While for the spectrum of the nanowalls, the dominative emission peak is the FX-1LO replica. The enhancement of phonon modes in the ZnO nanowalls could contribute to residual strain induced additional electron–phonon interaction, which enhance the signal associated with LO phonon. Similar phenomena have been observed in multiple-quantum-well [20] and superlattices structures [21]. The strain-generated electric fields, which occur in the multiple-quantum-well structures, induced additional electron–phonon interaction, which enhanced the signals related to phonon. The residual

J. Phys. D: Appl. Phys. **42** (2009) 135415

F Fang *et al*

strain in ZnO nanowalls may occur during the coalescence growth process (as shown in figure 3(*b*)), in which the *a*-axis orientation is stretched while the *c*-axis orientation is compressed. This deduction is in agreement with the XRD results. With the increase in temperature, the emission peaks moved towards the lower-energy side and gradually got broadened due to the LO phonon scattering and increased exciton thermal ionization [22]. The exciton-related emissions of the ZnO nanowalls are quenched so fast that they could not be observed above 180 K. This result suggested that the UV emission of the ZnO nanowalls originated mainly from FX-LO phonon replicas. For ZnO nanowires the near band-edge emission at room temperature is a dual contribution of FX and FX-LO-phonon. For this reason the photon emission peak of the ZnO nanowalls shifts to the low energy side at room temperature as shown in figure 4.

In conclusion, vertically aligned ZnO nanowires and nanowalls were grown on the Si substrate by a carbonthermal reaction utilizing a thin ZnO film to promote nucleation and control the growth orientation. The incoming gas flow is a critical experimental parameter for the formation of different morphologies of ZnO nanostuctures. Apart from the different morphologies, the photoluminescence of both nanostructures also showed a significant distinction. The PL and XRD results suggested that the residual strain in ZnO nanowalls during the coalescence growth process induced an additional channel of electron–phonon coupling, which enhanced the signal associated with the LO phonon significantly.

Acknowledgments

References

[1] Cui Y, Wei Q Q, Park H K and Lieber C M 2001 *Science* **293** 1289
[2] Lee C J, Lee T J, Lyu S C, Zhang Y and Lee H J 2002 *Appl. Phys. Lett.* **81** 3648
[3] Wang Z L 2003 *AdV. Mater.* **15** 43
[4] Huang M H, Mao S, Feick H, Yan H, Wu Y, Kind H, Weber E, Russo R and Yang P 2001 *Science* **292** 1897
[5] Pan Z W, Dai Z R and Wang Z L 2001 *Science* **291** 1947
[6] Park W I, KimD H, Jung S W and Yi G C 2002 *Appl. Phys. Lett.* **80** 4232
[7] Wu J J, Liu S C, Wu C T, Chen K H and Chen L C 2002 *Appl. Phys. Lett.* **81** 131
[8] Kim S W, Fujita S, Yi M S and Yoon D H 2006 *Appl. Phys. Lett.* **88** 253114
[9] Kim S W, Park H K, Yi M S, Park N M, Park J H, Kim S H, Maeng S L, Choi C J and Moon S E 2007 *Appl. Phys. Lett.* **90** 033107
[10] Zhang B P, Wakatsuki K, Binh N T and Segawa Y J 2004 *Appl. Phys.* **96** 340
[11] Ng H T, Li J, Smith M K, Nguyen P, Cassell A, Han J and Meyyappan M 2003 *Science* **300** 1249
[12] Grabowska J, Meaney A, Nanda K K, Mosnier J P, Henry M O, Duclère J R and Mcglynn E 2005 *Phys. Rev. B* **71** 115439
[13] Li C, Fang G, Su F, Li G, Wu X and Zhao X 2006 *Nanotechnology* **17** 3740
[14] Fang F, Zhao D X, Zhang J Y, Shen D Z, Lu Y M, Fan X W, Li B H and Wang X H 2007 *Nanotechnology* **18** 235604
[15] Song J H, Wang X D, Riedo E and Wang Z L 2005 *J. Phys. Chem. B* **109** 9869
[16] Dalal S H, Baptista D L, Teo K B and Lacerda R G 2006 *Nanotechnology* **17** 4811
[17] Vanheusden K, Warren W L, Sesger C H, Tallant D R, Voigt J A and Gnage B E 1996 *J. Appl. Phys.* **79** 7983
[18] Yao D B, Chan Y F and Wang N 2002 *Appl. Phys. Lett.* **81** 757
[19] Liang W Y and Yoffe A D 1968 *Phys. Rev. Lett.* **20** 59
[20] Sela I and Smith D L 1992 *Phys. Rev. B* **46** 1480
[21] Rozas G, Pascual, Winter M F, Fainstein A, Jusserand B, Vaccaro P O and Saravanan S 2008 *Phys. Rev. B* **77** 165314
[22] Makino T, Chia C H, Tuan N T, Segawa Y, Kawassaki M, Ohtomo A, Tamura K and Koinuma H 2000 *Appl. Phys. Lett.* **76** 3549